

HD344787: a true Polaris analogue? [★]

V. Ripepi¹, G. Catanzaro², L. Molnár^{3,4,5}, E. Plachy^{3,4}, M. Marconi¹, G. Clementini⁶, R. Molinaro¹,
G. De Somma^{1,7,8}, S. Leccia¹, S. Mancino^{9,10,11}, I. Musella¹, F. Cusano⁶, and V. Testa¹²

¹ INAF-Osservatorio Astronomico di Capodimonte, Salita Moiariello 16, 80131, Naples, Italy
e-mail: vincenzo.ripepi@inaf.it

² INAF-Osservatorio Astrofisico di Catania, Via S.Sofia 78, 95123, Catania, Italy
e-mail: giovanni.catanzaro@inaf.it

³ Konkoly Observatory, ELKH Research Centre for Astronomy and Earth Sciences, Konkoly Thege 15-17, H-1121 Budapest, Hungary

⁴ MTA CSFK Lendület Near-Field Cosmology Research Group

⁵ ELTE Eötvös Loránd University, Institute of Physics, 1117, Pázmány Péter sétány 1/A, Budapest, Hungary

⁶ INAF-Osservatorio di Astrofisica e Scienza dello Spazio, Via Gobetti 93/3, I-40129 Bologna, Italy

⁷ Dipartimento di Fisica "E. Pancini", Università di Napoli "Federico II", Via Cinthia, 80126 Napoli, Italy

⁸ Istituto Nazionale di Fisica Nucleare (INFN)-Sez. di Napoli, Via Cinthia, 80126 Napoli, Italy

⁹ European Southern Observatory, Karl-Schwarzschild-Strasse 2, D-85748 Garching bei München, Germany

¹⁰ Cluster of Excellence Universe, Technical University of Munich, Boltzmannstr 2, D-85748 Garching, Germany

¹¹ Ludwig-Maximilians-Universität München, Physics Department, Geschwister-Scholl-Platz 1, D-80539 München, Germany

¹² INAF – Osservatorio Astronomico di Roma, via Frascati 33,

ABSTRACT

Context. Classical Cepheids (DCEPs) are the most important primary indicators for the extragalactic distance scale, but they are also important objects per se, allowing us to put constraints on the physics of intermediate-mass stars and the pulsation theories.

Aims. We have investigated the peculiar DCEP HD 344787, which is known to exhibit the fastest positive period change among DCEPs along with a quenching amplitude of the light variation.

Methods. We have used high resolution spectra obtained with HARPS-N@TNG for HD 344787 and the more famous Polaris DCEP, to infer their detailed chemical abundances. Results from the analysis of new time-series photometry of HD 344787 obtained by the TESS satellite are also reported.

Results. The double mode nature of HD344787 pulsation is confirmed by analysis of the TESS light curve, although with rather tiny amplitudes of a few tens of millimag. This is indication that HD344787 is on the verge of quenching the pulsation. Analysis of the HARPS-N@TNG spectra reveals an almost solar abundance and no depletion of carbon and oxygen. Hence, the star appears to have not gone through first dredge-up. Similar results are obtained for Polaris.

Conclusions. Polaris and HD344787 are confirmed to be both most likely at their first crossing of the instability strip (IS). The two stars are likely at the opposite borders of the IS for first overtone DCEPs with metal abundance $Z=0.008$. A comparison with other DCEPs which are also thought to be at their first crossing allows us to speculate that the differences we see in the Hertzsprung-Russell diagram might be due to differences in the properties of the DCEP progenitors during the main sequence phase.

Key words. Stars: distances — Stars: variables: Cepheids — Stars: abundances — Stars: fundamental parameters — Stars: Individual: HD 344787 — Stars: Individual: Polaris

1. Introduction

Albeit primarily known for their fundamental role in the extragalactic distance scale, Classical Cepheids (DCEPs) through their pulsational properties also allow us to get insights into evolutionary properties and stellar interiors, hence, to put constraints on the physics of intermediate mass stars and pulsation theories (see e.g. Anderson et al. 2016; Bhardwaj et al. 2018; Marconi et al. 2020, and references therein).

In this context, particularly interesting are DCEPs showing rapidly increasing periods, as they are thought to be crossing the instability strip (IS) for the first time (see e.g. Turner et al. 2006). Polaris is the most famous among the DCEPs thought to be at

their first crossing. The star exhibits a fast increasing period with changes on the order of $4.4\text{--}4.9\text{ s yr}^{-1}$ (see e.g. Evans et al. 2002; Turner et al. 2005; Bruntt et al. 2008) along with abrupt variations (see Turner 2009). Polaris has also a peculiarly low and changing amplitude of the light variation, which decreased from ~ 0.1 mag, during most of the past century, to a few hundredths of magnitude in the early 2000's (e.g., Turner 2009). This amplitude is more typical of pulsators on the hot and cool edges of the strip, whereas Polaris was thought to be in the middle of the IS. According to Turner et al. (2013), Polaris observations can be explained if the stars is at its first crossing, taking into account that theoretical models by Alibert et al. (1999) predict a first crossing instability strip shifted blue-ward and, in general, the DCEPs instability strip tends to widen and gets redder as luminosity increases (see e.g. Bono et al. 2000; De Somma et al. 2020), allowing the convection to damp pulsation at hotter temperatures with respect to the other crossings. The red-ward path of Polaris

[★] Based on observations made with the Italian Telescopio Nazionale Galileo (TNG) operated by the Fundación Galileo Galilei (FGG) of the Istituto Nazionale di Astrofisica (INAF) at the Observatorio del Roque de los Muchachos (La Palma, Canary Islands, Spain).

toward the cool edge of the first crossing IS suggested by its constantly increasing period would thus also be consistent with its decreasing amplitude. However, Polaris has not ceased pulsating just yet. After its amplitude reached a minimum at around year 1990, it has been slowly increasing again (e.g. Bruntt et al. 2008; Turner 2009, see section 4 for more details on this point), although current radial velocity amplitudes have still not reached the levels measured in the first half of the 20th century (Usenko et al. 2018).

A further object with Polaris-like characteristics was discovered a decade ago by Turner et al. (2010), HD 344787. The star is a multi-mode DCEP, with fundamental (F) and first overtone (FO) periods of 5.4 days and 3.8 days, respectively. Study of the O–C diagram revealed that the F-mode period of HD 344787 is increasing by 12.96 ± 2.41 s yr $^{-1}$, one of the fastest period variations ever measured for a DCEP. According to Turner et al. (2010), such period variation is in agreement with the expectation of stellar evolution theory for a first-crossing, red-ward evolving DCEP. Even more striking is the similarity with Polaris for what concerns the light amplitude. Indeed, HD 344787 shows a quickly diminishing amplitude which decreased from ~ 0.05 mag (summing up F- and FO- amplitudes) in the first 20 years of the past century to become barely detectable around years 2008–2009. The waning amplitude would imply, even more than for it did for Polaris, that the star is leaving the instability strip, and HD 344787 is foreseen to soon completely cease pulsation, as the most recent observations collected by Turner et al. (2010) in 2010 found amplitudes compatible with non-variability (~ 2 – 3 mmag) from ground-based observations.

Notwithstanding the close similarity to Polaris and its clear relevance in the context of stellar evolution and pulsation theories, the study of HD 344787 have not progressed after the work by Turner et al. (2010). In this paper we carry forward the investigation of HD 344787, based on three new pieces of information: 1) high-precision photometry of HD 344787 by the TESS satellite (Ricker et al. 2015); 2) elemental abundances from high-resolution spectra obtained with the HARPS-N instrument on the TNG, and: 3) precise distances from the Gaia mission (Gaia Collaboration et al. 2018). The combination of these novel elements allows us to study in detail the pulsation properties of HD 344787 and, in turn, to precisely locate the star in the Hertzsprung–Russell diagram. This allows us to discuss the evolutionary status of HD 344787 in comparison with Polaris and other DCEPs thought to be first-crossing the IS, trying to explain the peculiarities shown by these stars.

Even if Polaris is the closest and brightest DCEP known so far, there are only a few chemical analyses of its atmosphere available in the literature. In particular, the latest parameter determinations (effective temperature, gravity, and abundances) date back to the paper by Usenko et al. (2005). In order to obtain an updated set of abundances, we retrieved high resolution spectra available for Polaris in the HARPS-N@TNG archive and, to ease the comparison with HD 344787, we analysed the spectra of both stars using exactly the same methodology (see Sect. 2.2).

The paper is organised as follows: Sect. 2 describes the spectroscopic observations and the data reductions. TESS photometry for HD 344787 is presented in Sect. 3. In Sect. 4 we discuss the comparison of H 344787 with Polaris. Finally, Sect. 5 presents a discussion of our results, whereas Sect. 6 summarises the paper conclusions.

Table 1. Atmospheric parameters. For each spectrum of HD 344787 we list heliocentric Julian Day (HJD) at mid exposure (column 1), effective temperature (column 2), gravity (column 3), micro-turbulent and radial velocities (columns 4 and 5).

HJD	T _{eff} (K)	log g (dex)	ξ (km s $^{-1}$)	v _{rad} (km s $^{-1}$)
2459000+				
29.51441	5750 ± 150	1.3 ± 0.2	3.0 ± 0.2	-8.67 ± 0.08
46.46831	5750 ± 110	1.3 ± 0.2	3.1 ± 0.2	-8.82 ± 0.09
53.71637	5750 ± 110	1.3 ± 0.2	3.0 ± 0.2	-8.75 ± 0.06

2. Spectroscopic observations

2.1. Observations and data reduction

Three spectroscopic observations of the Galactic DCEP HD 344787 were obtained at the 3.5m Telescopio Nazionale Galileo (TNG) equipped with the HARPS-N instrument, in the nights of June 28 and July 15 and 22, 2020. The spectra cover the wavelength range between 3830 to 6930 Å, with a spectral resolution $R=115,000$, and a signal-to-noise ratio (S/N) of about 100 at $\lambda 6000$ Å for each of them.

Reduction of all spectra, which included bias subtraction, spectrum extraction, flat fielding and wavelength calibration, was performed using the HARPS reduction pipeline. Radial velocities were measured by cross-correlating each spectrum with a synthetic template. The cross-correlation was performed using the IRAF task *FXCOR* and excluding Balmer lines and wavelength ranges including telluric lines. The IRAF package *RV-CORRECT* was used to determine heliocentric velocities, by correcting the spectra for the Earth's motion.

We retrieved two spectra of Polaris from the HARPS-N archive. Those spectra had been acquired consecutively on April, 22nd 2015, both of them has been taken with an exposure time of 20 sec, cover the wavelength range between 3830 to 6930 Å, with a spectral resolution $R=115,000$, and has signal-to-noise ratio (S/N) of about 250 at $\lambda 6000$ Å. Further, we combined them obtaining an S/N higher than 300 over the spectral range greater than $\lambda 4000$ Å.

2.2. Data analysis

Abundance analyses of HD 344787 and Polaris followed exactly the same procedure. Effective temperatures were estimated using the line depth ratios (LDRs) method (Kovtyukh & Gorlova 2000). LDRs have the advantage of being sensitive to temperature variations, but not to abundances and interstellar reddening. Typically, we measured about 32 LDRs in each spectrum.

To determine the micro-turbulent velocity ξ , iron abundance, and log g, we followed the iterative procedure recently outlined in Catanzaro et al. (2020). Briefly, micro-turbulence was deducted by the slope of iron abundances versus equivalent widths (EWs), while surface gravity was determined by imposing the ionisation balance between Fe I and Fe II lines (145 Fe I and 24 Fe II spectral lines were extracted from Romaniello et al. 2008). EWs were measured using an *IDL*¹ semi-automatic custom routine, which allowed us to minimise errors in the continuum evaluation on the wings of the spectral lines. Then they were converted to abundances by using the *WIDTH9* code (Kurucz & Avrett 1981) after generating an appropriate model atmosphere with the *ATLAS9 LTE* code (Kurucz 1993a,b). The atmospheric

¹ IDL (Interactive Data Language) is a registered trademark of Harris Geospatial Solutions

Table 2. Atmospheric parameters adopted for HD 344787 and Polaris.

Star	T_{eff} (K)	$\log g$ (dex)	ξ (km s^{-1})
HD 344787	5750 ± 120	1.3 ± 0.2	3.0 ± 0.2
Polaris	6000 ± 70	2.0 ± 0.2	2.8 ± 0.2

parameters derived for each spectrum of HD 344787 are summarised in Table 1. Since for the three spectra of HD 344787 we obtained quite consistent parameters, we combined them in a unique average spectrum with increased $S/N \approx 130$. For the subsequent abundance analysis we adopted for HD 344787 the average values reported in the upper line of Tab. 2. The lower line shows instead the parameter values we obtained for Polaris.

As a further check, we reproduced the observed spectral energy distributions (SEDs) with synthetic fluxes computed with the ATLAS9 code by using the parameters reported in Table 2. The observed fluxes were retrieved from the VOSA tool (Bayo et al. 2008), corrected for reddening by adopting $E(B-V) = 0.52 \pm 0.03$ mag (Kervella et al. 2019, for HD 344787) and $E(B-V) = 0.02 \pm 0.01$ mag (Turner et al. 2013, for Polaris), and the Fitzpatrick (1999) extinction law. In Fig. 1 we show the comparison between the observed and the theoretical SEDs. The upper panel refers to HD 344787, where we excluded WISE photometry due to contamination by a close cool star, while the bottom panel shows Polaris.

Furthermore, using the distance inferred from the *Gaia* DR2 parallax ($\varpi = 0.6865 \pm 0.0355$ mas, to which we applied a zero-point correction of 0.049 mas; Groenewegen 2018), we derived an absolute luminosity of $L/L_{\odot} = 1435 \pm 147$ for HD 344787. For Polaris, we adopted the distance by Hipparcos ($D = 133 \pm 2$ pc), obtaining $L/L_{\odot} = 2540 \pm 366$.

The radial velocity values listed in column 5 of Table 1 were calculated by cross-correlating each observed spectrum with a synthetic template as described in the previous section. The three values are practically identical within the errors and this could be interpreted as a vanishing amplitude of the pulsation, thus supporting a first crossing of the IS by HD 344787. However, the almost identical radial velocities could also arise if the 3 spectra had been taken at same pulsation phase by chance. Using the pulsation modes (see Sect. 3) we computed an artificial light curve of HD 344787 covering the time interval containing the Julian Dates of our spectroscopic observations. This allowed us to verify that the spectrum taken at $\text{HJD} = 2459046.46831$ is close to a minimum of the HD 344787 light curve, whereas the spectrum observed at $\text{HJD} = 2459053.71637$ is close to a maximum. We can thus conclude that the almost null amplitude of the radial velocity variation of HD 344787 is real.

Finally, the atmospheric parameters reported in Table 2 were used as input for the abundance analysis, which was performed following the procedures outlined in Catanzaro et al. (2019). The total line broadening, estimated by using metal lines, is of 12 ± 1 km s^{-1} for both stars. The abundances of the 28 species we detected in the spectra are provided in Table 3 and plotted with different symbols in Fig. 2. HD 344787 and Polaris have chemical patterns fully consistent within the errors.

Our elemental abundances for Polaris, can be compared with those derived by Usenko et al. (2005). The only two differences concern magnesium and strontium. For Usenko et al. (2005) magnesium is under-abundant by ≈ 0.2 dex in comparison with the Sun, while we derived an overabundance of ≈ 0.2 dex, and strontium is overabundant by about 0.4 dex for Usenko et al. (2005) while we found it to be consistent with the solar value.

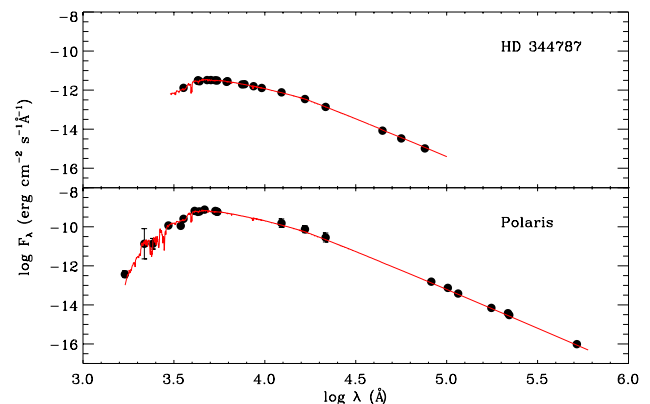


Fig. 1. Spectral energy distribution of HD 344787 (upper panel) and Polaris (bottom panel). Filled dots represent the observed fluxes as retrieved from the VOSA tool. The red line shows the theoretical flux computed using the ATLAS9 code.

Table 3. Derived abundances for HD 344787 and Polaris expressed in terms of solar values (Grevesse et al. 2010).

El	HD 344787 [X/H]	Polaris [X/H]
C	-0.09 ± 0.11	-0.05 ± 0.15
O	0.07 ± 0.14	0.09 ± 0.20
Na	0.16 ± 0.18	0.18 ± 0.16
Mg	0.05 ± 0.13	0.18 ± 0.12
Al	0.08 ± 0.18	0.01 ± 0.15
Si	0.00 ± 0.14	0.06 ± 0.13
S	0.09 ± 0.11	0.12 ± 0.11
Ca	0.00 ± 0.13	0.00 ± 0.12
Sc	0.07 ± 0.08	0.09 ± 0.15
Ti	-0.03 ± 0.15	0.08 ± 0.17
V	-0.05 ± 0.17	0.05 ± 0.10
Cr	-0.03 ± 0.19	0.08 ± 0.15
Mn	0.01 ± 0.16	0.05 ± 0.11
Fe	-0.06 ± 0.10	0.03 ± 0.13
Co	0.05 ± 0.17	0.00 ± 0.14
Ni	-0.08 ± 0.20	-0.09 ± 0.17
Cu	-0.08 ± 0.15	0.02 ± 0.09
Sr	0.03 ± 0.20	0.09 ± 0.15
Y	0.00 ± 0.10	0.12 ± 0.15
Zr	0.10 ± 0.11	0.07 ± 0.11
Ba	0.22 ± 0.10	0.25 ± 0.17
La	0.03 ± 0.15	0.00 ± 0.15
Ce	0.15 ± 0.15	0.10 ± 0.15
Pr	-0.28 ± 0.15	-0.18 ± 0.15
Nd	0.00 ± 0.15	-0.03 ± 0.15
Sm	-0.00 ± 0.15	-0.12 ± 0.15
Eu	-0.13 ± 0.15	-0.08 ± 0.15
Gd	0.00 ± 0.15	-0.03 ± 0.15

For all other species both analyses gave consistent results within the errors.

3. TESS photometry

HD 344787 was recently observed by the Transiting Exoplanet Survey Satellite (TESS). TESS was built to perform a nearly all-sky survey providing high-precision continuous photometric data that ranges from 27 days up to 351 days in length, depending on celestial position (Ricker et al. 2015). The southern eclips-

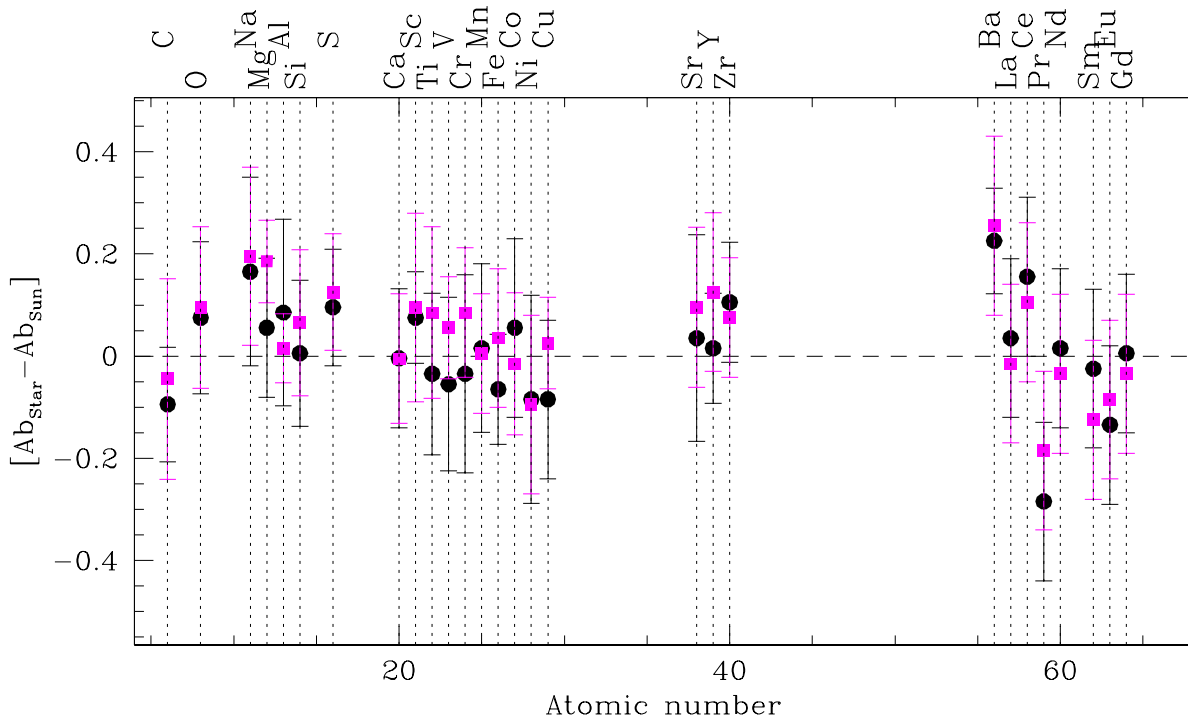


Fig. 2. Chemical pattern for HD 344787 (black filled dots) and Polaris (magenta filled squares) with abundances plotted in terms of solar values (Grevesse et al. 2010).

tic hemisphere was monitored in the first year of the mission, dividing the field of view into 13 overlapping sectors and rotating around the ecliptic pole. The telescope then turned to the northern ecliptic hemisphere in the second year, and observed HD 344787 in Sector 14. The star has a brightness of 8.1 mag in the TESS pass-band, which spans the 600–1000 nm wavelength range and is centred on the Cousins I band. At this brightness \sim 100 ppm photometric precision per 30-min cadence is achievable with TESS, however, instrumental issues strongly affect the data quality at certain observing times and positions within the field of view (Huang et al. 2020).

3.1. TESS light curve extraction

HD 344787 was pre-selected to be observed in 2-minute cadence mode. These observations are made through small sub-images centred on the targets, and for them photometric data are available at the Mikulski Archive, as provided by the TESS Science Processing Operations Center (SPOC). Unfortunately, no intrinsic variability could be detected in the SPOC light curve beyond a 20–30 mmag scatter, but it became evident that the star is affected by both stray light and by reflections from the metal straps of the electronics behind the CCD. Therefore we generated differential-image photometry with the FITSH package from the full-frame images that were taken with 30-minute cadence. The reduction process corrects many of the instrumental issues (differential velocity aberration, spacecraft jitters, background and stray light variations, strap reflection, etc.) and we found it to be extremely useful in previous studies of TESS variables (see, e.g., Borkovits et al. 2020; Merc, J. et al. 2020; Szegedi-Elek et al. 2020). The pipeline also allows us to adjust the aperture size of the photometry, which is often critical in more crowded areas. TESS operates with a relatively small, 21 $''$ /px spatial resolution that results in significant contamination by nearby stars, especially in the denser stellar fields. Our pre-

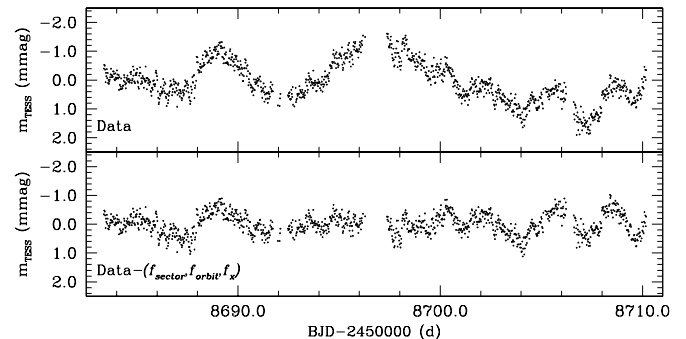


Fig. 3. TESS light curve of HD344787, as derived from the full-frame images with the FITSH differential image photometry pipeline. The top panel shows the light curve in mmag after subtracting the average value ($m_{TESS} = 8.1055$ mag); the bottom panel shows the light curve after removing the first three instrumental frequencies (see Table 4).

vious tests indicated that an aperture with a 2.5 px radius works well for most of the stars, and we used that value for HD 344787 as well. Our photometric solution is displayed in Fig. 3. It is immediately clear from the light curve that any variation present has very small amplitude.

3.2. Frequency analysis

We performed a standard Fourier analysis with the Period04 software (Lenz & Breger 2005) that revealed 7 frequencies in the data with a signal to noise ratio (S/N) greater than 4. If we allow a lower limit ($S/N > 3$), one more frequency can be detected. The frequency content is displayed in Table 4 and graphically shown in Fig. 4. Multiple of the highest-amplitude frequencies have instrumental origins: we identified both the periodicity of TESS's orbit (13.7 days) and length of a TESS sector (27.4 d, consisting

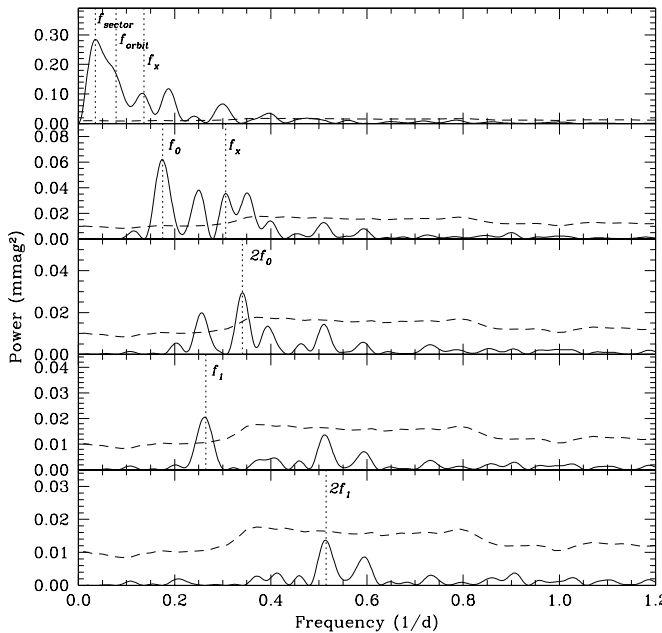


Fig. 4. Periodogram of HD344787 from TESS data. The different panels show the frequencies labeled in Table 4. The dashed line represents the level of noise.

of two orbits). The existence of these frequencies shows that our photometric pipeline could not entirely eliminate instrumental issues, only reduce them to the mmag level. The double-mode pulsation causes a weaker, but still detectable signal in the TESS data: we found both the fundamental mode (f_0) and the first overtone mode (f_1), according to the classification in the literature (see Turner et al. 2010), along with the first harmonic frequencies ($2f_0$ and $2f_1$). Both modes have shown decreasing amplitudes in the historical data of HD 344787 (Fig. 8 in Turner et al. 2010), but even with the uncertainties, variation in the amplitudes is noticeable and the fundamental mode occasionally exceeds the overtone mode which normally dominates in the light variation. This happened again during the TESS observations, where we detected Fourier amplitudes twice as strong for the fundamental mode than for the overtone. We also found the additional frequency, f_x , and a possible combination frequency with f_0 ($f_0 + f_x$). The notation x indicates that we are uncertain about the origin of this frequency, however, given the low resolution of the TESS images, it is likely caused by blending. Interestingly, f_x is close to the value of $0.5f_1$. Finally, we note that the period ratio of the main radial modes of HD 344787 is $P_0/P_1 \sim 0.70$ (Turner 2009). Considering that $P_0 \sim 5.4$ days, the position of the star in the Petersen diagram is in the expected region for Galactic DCEPs pulsating in both fundamental and first overtone mode, as can be seen in Fig. 5.

4. HD 344787 vs Polaris

The two DCEPs addressed in our paper can be compared from different points of view and perspectives:

- **Position in the Hertzsprung-Russell diagram (HRD):** The T_{eff} and luminosity values derived in Sect. 2.2 have been used to locate HD 344787 and Polaris on the HRD, as shown in Fig. 6. The figure includes the ISs for fundamental mode and first overtone DCEPs with metal abundances $Z=0.02$ (De Somma et al. 2020) and $Z=0.008$ (Bono et al. 2001),

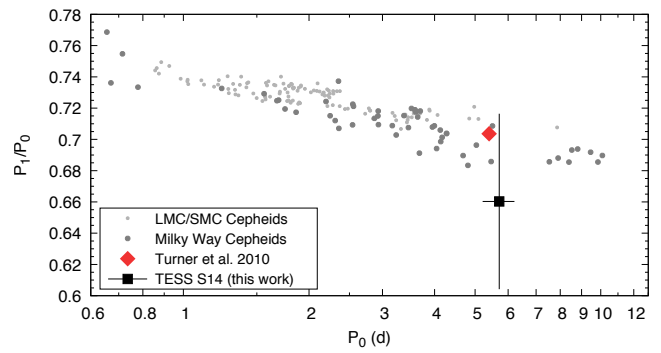


Fig. 5. Petersen diagram of double-mode DCEPs pulsating in fundamental mode and the first overtone, with the period ratios of HD344787 measured by Turner et al. (2010) (red diamond) and in this work (black square). Data for other Galactic DCEPs are from Udalski et al. (2018) and Jurcsik et al. (2018). Data for DCEPs in the Large and Small Magellanic Clouds come from Soszyński et al. (2015).

Table 4. Results of the frequency analysis of HD 344787 based on TESS data obtained in Sector 14.

ID	Frequency (1/d)	Period d	Amplitude (mmag)	S/N
f_{sector}	0.035	28.6 ± 1.6	0.56	32.6
f_{orbit}	0.078	12.8 ± 0.7	0.68	40.5
f_x	0.136	7.4 ± 0.4	0.56	31.3
f_0	0.175	5.7 ± 0.5	0.29	14.3
$f_0 + f_x$	0.306	3.3 ± 0.2	0.18	8.2
$2f_0$	0.341	2.9 ± 0.1	0.20	6.9
f_1	0.265	3.8 ± 0.2	0.16	7.8
$2f_1$	0.515	1.9 ± 0.1	0.12	3.9

respectively. These values bracket the metallicity of the Sun used here, $Z=0.0152$, according to the PARSEC evolutionary tracks by Bressan et al. (2012) which are also displayed in the figure (for $Z=0.014$, $Y=0.273$) as a reference for the typical masses expected from stellar evolution. The position in the HRD of the two stars is close but, thanks to the small errors, significantly different both in luminosity and T_{eff} . According to Anderson (2018) Polaris is a $7 M_{\odot}$ star at the hot boundary of the first crossing IS. This seems confirmed by the star location in the HRD (see Fig. 6), very close to the First Overtone Blue Edge (FOBE) of the $Z=0.008$ IS predicted by pulsation models, with a mass of about $6 M_{\odot}$. Our lower mass estimate is mainly due to the different parallax value adopted here (7.54 ± 0.11 mas, van Leeuwen 2007), than in Anderson (2018) who adopted the parallax of Polaris B measured with the HST (6.26 ± 0.24 mas, Bond et al. 2018). Our choice is also in very good agreement with the parallax of Polaris B as published by Gaia DR2, $\varpi = 7.292 \pm 0.028$ mas and EDR3 (early data release 3 Gaia Collaboration et al. 2016, 2020), $\varpi = 7.2869 \pm 0.0178$ mas. On this basis, the position of Polaris on the HRD appears rather accurate and is not compatible with the very low dynamical mass $3.5 \pm 0.8 M_{\odot}$ measured by Evans et al. (2018) through the analysis of Polaris system orbit (see also their detailed discussion about the mass of Polaris in comparison with that of the binary DCEP V1334 Cyg, accurately measured by Gallenne et al. 2018). However, the same Authors state that more data is needed to better define Polaris' orbit. Therefore, its dynamical

Table 5. Adopted effective temperatures and luminosities for the stars discussed in Sect. 5.

Star	$T_{eff}(K)$	L/L_\odot	Source
HD 344787	5750±150	1435±147	This Work
Polaris	6000±100	2540±340	This Work
BY Cas	6000±265	1700±41	Groenewegen (2020) ^a
SZ Cas	5250±290	4607±1100	Groenewegen (2020) ^a
RU Sct	5000±221	8367±2844	Groenewegen (2020) ^a
ASAS 075842-2536.1	6300±100	126±58	Catanzaro et al. (2020)
ASAS 131714-6605.0	6300±100	640±170	Catanzaro et al. (2020)
V1033 Cyg	5860±100	742±192	Catanzaro et al. (2020)
V371 Per	6000±100	949±668	Catanzaro et al. (2020)
V363 Cas	6680±110	257±48	Catanzaro et al. (2020)

Notes. a = the uncertainty in luminosity was increased with respect to the original value to include the error on *Gaia* DR2 parallax.

cal mass estimate could actually be consistent with the evolutionary one.

The position of HD 344787 appears to be redder and fainter than Polaris, indicating a slightly lower mass, on the order of 5.3-5.5 M_\odot . More in detail, HD 344787 is placed slightly off the first overtone red edge (FORE) for $Z=0.008$, and just above the intersection with the fundamental blue edge (FBE) for $Z=0.02$. This location is in agreement with both the star pulsation to be vanishing and HD 344787 to be a multi-mode (F/FO) pulsator. Therefore, the difference in T_{eff} between the two DCEPs (albeit significant only at $\sim 1\sigma$ level), allows us to estimate the width of the first overtone IS, i.e. $\Delta T_{eff} \sim 250$ K (in good agreement with theoretical predictions by Bono et al. 2001).

– **Pulsation properties:** The pulsation mode of Polaris has long been debated in the literature. However, Anderson (2018) convincingly showed that the FO pulsation mode should be preferred than the F-mode (as proposed by, e.g. Turner et al. 2013) or the second overtone (2O) mode (see Bond et al. 2018). As pointed out in Sect. 1, the period of Polaris is increasing at a high rate, and even after the so called "glitch" occurred around 1965 (Turner 2009; Turner et al. 2013), when the rate of increase has slightly shortened, its positive increment remains compatible with a red-ward evolving star in the HRD, crossing the IS for the first time. Polaris' light pulsation amplitude prior to the 1965 glitch showed a slow but steady abatement, with an abrupt decline after this event, reaching a minimum amplitude in V band of ~ 0.025 mag around 1988 (Turner 2009). It is presently slightly increasing (Bruntt et al. 2008; Turner 2009; Turner et al. 2013), but might vanish completely in a couple thousand years if the pre-glitch trend continues (Turner 2009). Also the current radial velocity amplitudes are not back again at the levels measured before the glitch (Usenko et al. 2018). Concerning the "glitch", which corresponds to a sudden drop in pulsation period, according to Turner (2009) it could be explained by the quick acquisition of about seven Jovian masses by Polaris. This fascinating scenario is not so remote, as the observations of the last two decades from both ground and space have revealed that extra-solar planets are very common. Interestingly, the possible assimilation of planetary companion(s) for an intermediate-mass star like Polaris, is expected to happen during the first crossing of the IS, i.e. the evolutionary phase when the star expands its envelope for the first time to become a red super-giant.

As for HD 344787, the TESS data confirm excitation of two frequencies in the star, which Turner et al. (2010) had iden-

tified as F and FO pulsation modes. Similarly to Polaris, the star shows a very fast period increase and diminishing amplitude, which is barely detectable only thanks to high precision of TESS data.

This complex observational scenario shows that Polaris and HD 344787 have indeed close similarities but also remarkable differences. Both stars have quickly increasing periods, which can naturally be explained by them being at the first crossing of the IS and evolving red-ward in the HRD. The diminishing pulsation amplitudes, is more striking in HD 344787, whose pulsation is still detectable only thanks to TESS precise photometry, whereas the amplitude of Polaris as remarked earlier, has a complex behaviour and, on top of a secular abatement, it is now slightly increasing. An alternative explanation of these observations comes from the suggestion that in general, overtone pulsators might have unusually large period changes (Szabados 1983). Adding to this the discontinuous amplitude variation, it can be hypothesised a phenomenon related to pulsation instead of only evolution. A possible connection between pulsation and period/amplitude change could be a high-rate of pulsation-induced mass loss. However, as noted by Evans et al. (2018) at moment there are no significant evidences of mass loss driven by pulsation in Polaris, whereas we have no data for HD 344787. The question whether or not the rapid period change in both Polaris and HD 344787 is just an extreme example of overtone pulsation instead of rapid evolution in the first instability strip crossing is an important one and requires further dedicated observations.

If the first crossing of the IS explains the similarities between Polaris and HD 344787, their diverse position in the HRD accounts for the differences. In fact, Polaris is still rather close to the FOBE and evolving towards the FORE, in a region of the IS where a very narrow FO zone is expected, according to pulsation models, while HD 344787 is likely between the FBE and the FORE, in a region of the IS where multi-mode pulsation is expected. The fast red-ward evolution in the HRD in the case of HD 344787 seems to lead the star to not only exit the FO IS but also the F-mode IS and quit pulsation, as testified by the almost undetectable pulsation, thus suggesting a position of the FRE very close to the FORE. This occurrence is not confirmed by the theoretical boundaries plotted in Fig. 6, where HD 344787 seems significantly bluer than the predicted FRE for both the considered chemical compositions. However, as suggested by a number of theoretical investigations devoted to the effect of super-adiabatic convection on the position of the DCEPs IS boundaries (see e.g. Fiorentino et al. 2007; De

Somma et al. 2020, and references therein), the assumed convective efficiency, that should be reasonably increased in the red part of the IS, significantly affect the position of the FRE. In particular this extreme boundary gets bluer by about 300 K as the mixing length parameter adopted in the pulsation code increases from 1.5 to 1.8 or 1.9. This blue-ward shift would be enough to locate HD 344787 very close to the predicted FRE.

– Chemical composition:

The chemical patterns of the two stars are quite similar. Within uncertainties, all the species show similar content. Abundances are also very consistent with solar standard values, at least within the experimental errors. In particular, carbon and oxygen have normal abundance and this could be interpreted as a further sign of first crossing DCEPs. In fact, the criterion usually adopted for spectroscopic identification of such objects is to search for stars whose chemical composition does not reflect changes induced by the first dredge-up (1DU, hereafter), which occurs later during the post-main sequence evolution of intermediate mass stars. When 1DU takes place, it brings incomplete CNO-cycle processed material from the inner layers to the stellar surface, modifying the initial atmospheric abundances of the CNO elements. In particular, carbon becomes deficient with respect to its initial abundance $[C/H] = -0.3$, nitrogen overabundant $[N/H] = 0.3$, while oxygen should remain practically unchanged (Luck et al. 2001, and references therein). Unfortunately, we do not have in our spectral range the typical nitrogen lines used in DCEPs (i.e. $N\lambda\lambda 7463.3\text{ \AA}$ and 8629.16 \AA), hence, we can base our conclusions only on carbon and oxygen. We did not find any peculiar signature in our spectra being carbon and oxygen departures from solar values negligible. We conclude in favour of first crossing phase for both HD 344787 and Polaris. It is worth noting that the evolutionary phase of Polaris is debated and controversial in the literature. Usenko et al. (2005) from their abundances analysis concluded that Polaris is probably at its third crossing of the IS. A similar conclusion was reported by Evans et al. (2018), as they stated that Polaris' abundances are compatible with a post 1st-DUP scenario. On the contrary, Anderson (2018) based on the abundances is in favor of our conclusion that Polaris is reaching the IS for the first time.

5. Discussion

In the previous section we have compared Polaris and HD 344787 to each other. Now, we compare their properties with the characteristics of other DCEPs which are suspected to be crossing the IS for the first time. We can divide them in two groups with different characteristics. The first group is composed by objects with significant positive increase of the period and, in addition to Polaris and HD 344787, includes the FO-mode DCEP: BY Cas² (see, e.g. Turner et al. 2010; Berdnikov 2019a, and references therein) and the two F-mode DCEP: SZ Cas and RU Sct (see, e.g. Usenko & Klochkova 2015, and references therein).

The second group is composed by DCEPs whose spectra show the $Li\lambda 6707.766\text{ \AA}$ line. This feature is associated

with a first crossing of the IS as lithium is expected to be destroyed by proton-capture after the first dredge-up, i.e. at the beginning of the Red Giant Branch (RGB) phase (Iben 1967). Five stars with such characteristics are known so far in our Galaxy: ASAS J075842-2536.1, ASAS J131714-6605.0, V371 Per, V1033 Cyg and V363 Cas (Luck & Lambert 2011; Kovtyukh et al. 2016, 2019; Catanzaro et al. 2020). DCEPs belonging to the two groups are also displayed on the HRD in Fig. 6 using the effective temperatures and luminosities listed in Table 5. An inspection of Fig. 6 reveals that among the DCEPs which are candidates for first crossing, those showing Li lines in their spectra appear to be significantly less luminous. If all DCEPs shown in Fig. 6 are indeed first crossing the IS³, the under-luminosity of the Li rich DCEPs might suggest that mass drives the presence or not of Li in DCEP spectra. On the other hand, 1DU is not the only mechanism potentially able to deplete lithium, as rotational mixing can deplete Li abundance to 1% in a fraction of the main sequence (MS) lifetime, if the star is rotating fast enough during the MS phase (e.g. Brott et al. 2011). On this basis, even if statistics is still poor, we could tentatively explain the difference between Li-rich and Li-depleted, candidate first crossing DCEPs in terms of mass and rotational velocity of the MS progenitors, being the former generally less massive and less rotating than the latter, which include the two stars discussed in this paper, HD 344787 and Polaris.

6. Conclusions

In this paper we have thoroughly investigated HD344787, a DCEP defined by Turner et al. (2010) as "a Polaris analogue that is even more interesting than Polaris". We analysed proprietary HARPS-N@TNG high resolution spectra of HD 344787 along with archival spectra of Polaris obtained with the same instrumental setup. We have found that the chemical pattern of HD 344787 is compatible with the solar one, also for the carbon and oxygen abundances. This is a first hint that the star has not undergone the 1DU, hence likely is at the first passage of the IS. Very similar results were found from the analysis of Polaris, even if it is important to note that the evolutionary status, age, and mass of this important star are still a matter of debate in the recent literature.

As for the pulsation properties of HD 344787, an analysis of the light curve observed by TESS has allowed us to confirm Turner et al. (2010)'s prediction that the very fast period increase along with the significant light amplitude decrease both point toward a vanishing pulsation in HD 344787. Indeed, the frequency analysis of the TESS light curve shows that the pulsation of both F- and FO-modes is at the level of only a few tens of mmag, measurable only from space. Consistently, no significant variation of the radial velocity is measured in our spectra within the uncertainties ($\sim 100\text{ m/s}$). The observational evidences we have gathered on HD 344787 can be explained if the star is on the verge of crossing the FORE boundary and, almost simultaneously the FRE, where convection is expected to damp pulsation. This implies that the predicted FRE location displayed in Fig. 6 should be revised increasing the efficiency of super-adiabatic

² The other DCEP traditionally considered to be a first crossing candidate along with BY Cas is DX Gem. However, Berdnikov (2019b) recently showed that the period of DX Gem is actually decreasing, hence the star is now considered a second crossing candidate.

³ The presence of Li in ASAS 131714-6605.0 can be explained in a different way, as this star does indeed show CNO abundances as it had already gone through the 1DU.

convection in this red part of the IS, in agreement with previous suggestions (see e.g. Fiorentino et al. 2007; De Somma et al. 2020, and references therein). In this respect HD 344787 differs from Polaris, which is bluer by some 250 K and more likely close to the FOBE while crossing the IS for the first time.

A comparison with other DCEPs which are thought to be first-crossing the IS suggests that these objects can be divided into two groups, depending on whether they show or not lithium in their atmospheres. This separation reflects a different position of each group in the HRD, with lithium-rich DCEPs being systematically fainter than lithium-depleted DCEPs. Since lithium can be destroyed in the MS by rotational mixing, we speculate that the difference between the two groups hints to different MS progenitors, being lithium-rich DCEPs the descendant of less massive, slowly rotating B-stars in the MS. These results must be corroborated by more statistically significant samples which will become available in the near future thanks to spectroscopic surveys that will be carried out with forthcoming high-resolution, multi-object spectrographs such as WEAVE@WHT (Dalton et al. 2012), 4MOST@VISTA (de Jong et al. 2012) and MOONS@VLT (Cirasuolo et al. 2014).

Acknowledgements. We wish to thank the anonymous Referee for their suggestions, which helped us to improve the paper. We wish to thank the whole staff of the TNG for their strenuous efforts in carrying out the observations even in this difficult pandemic time. This work has made use of data from the European Space Agency (ESA) mission *Gaia* (<https://www.cosmos.esa.int/gaia>), processed by the *Gaia* Data Processing and Analysis Consortium (DPAC, <https://www.cosmos.esa.int/web/gaia/dpac/consortium>). Funding for the DPAC has been provided by national institutions, in particular the institutions participating in the *Gaia* Multilateral Agreement. In particular, the Italian participation in DPAC has been supported by Istituto Nazionale di Astrofisica (INAF) and the Agenzia Spaziale Italiana (ASI) through grants I/037/08/0, I/058/10/0, 2014-025-R.0, and 2014-025-R.1.2015 to INAF (PI M.G. Lattanzi). This paper includes data collected by the TESS mission. Funding for the TESS mission is provided by NASA's Science Mission Directorate. The research leading to these results has been supported by the Lendület LP2014-17 and LP2018-7/2020 grants of the Hungarian Academy of Sciences. L.M. was supported by the Premium Postdoctoral Research Program of the Hungarian Academy of Sciences. This research made use of NASA's Astrophysics Data System.

References

Alibert, Y., Baraffe, I., Hauschildt, P., et al. 1999, *A&A*, 344, 551
 Anderson, R. I., Saio, H., Ekström, S., et al. 2016, *A&A*, 591, A8
 Anderson, R. I. 2018, *A&A*, 611, L7
 Bayo, A., Rodrigo, C., Barrado y Navascués, D., Solano, E., Gutiérrez, R., Morales-Calderón, M., Allard, F. 2008, *A&A* 492, 277B.
 Berdnikov, L. N. 2019a, *Astronomy Letters*, 45, 593
 Berdnikov, L. N. 2019b, *Astronomy Letters*, 45, 435.
 Bond, H. E., Nelan, E. P., Remage Evans, N., et al. 2018, *ApJ*, 853, 55
 Bono, G., Castellani, V., & Marconi, M. 2000, *ApJ*, 529, 293
 Bono, G., Gieren, W. P., Marconi, M., et al. 2001, *ApJ*, 563, 319
 Borkovits, T., Rappaport, S. A., Hajdu, T., et al. 2020, *MNRAS*, 493, 5005
 Bressan, A., Marigo, P., Girardi, L., et al. 2012, *MNRAS*, 427, 127
 Brott, I., de Mink, S. E., Cantiello, M., et al. 2011, *A&A*, 530, A115
 Bruntt, H., Evans, N. R., Stello, D., et al. 2008, *ApJ*, 683, 433
 Bhardwaj, A., Marconi, M., Kanbur, S., et al. 2018, *The Galactic Bulge at the Crossroads*, 3.
 Catanzaro, G., Ripepi, V., Clementini, G., et al. 2020, *A&A*, 639, L4
 Catanzaro, G., Busá, I., Gangi M., Giarrusso, M., Leone, F., Munari, M., 2019, *MNRAS*, 484, 2530
 Cirasuolo, M., Afonso, J., Carollo, M., et al., 2014, *Proc. SPIE*, 9147, id. 91470N
 Dalton, G., Trager, S. C., Abrams, D. C., et al., 2012, *Proc. SPIE*, 8446, id. 84460P
 de Jong, R. S., Bellido-Tirado, O., Chiappini, C., et al., 2012, *Proc. SPIE*, 8446, id. 84460T
 De Somma, G., Marconi, M., Molinaro, R., et al. 2020, *ApJS*, 247, 30
 Evans, N. R., Sasselov, D. D., & Short, C. I. 2002, *ApJ*, 567, 1121
 Evans, N. R., Karovska, M., Bond, H. E., et al. 2018, *ApJ*, 863, 187. doi:10.3847/1538-4357/aad410
 Fiorentino, G., Marconi, M., Musella, I., et al. 2007, *A&A*, 476, 863. doi:10.1051/0004-6361:20077587
 Fitzpatrick, E., 1999, *PASP*, 111, 63
 Gaia Collaboration, Prusti, T., de Bruijne, J. H. J., et al. 2016, *A&A*, 595, A1. doi:10.1051/0004-6361/201629272
 Gaia Collaboration, Brown, A. G. A., Vallenari, A., et al. 2018, *A&A*, 616, A1
 Gaia Collaboration, Brown, A. G. A., Vallenari, A., et al. 2020, *A&A*, arXiv:2012.01533
 Gallenne, A., Kervella, P., Evans, N. R., et al. 2018, *ApJ*, 867, 121. doi:10.3847/1538-4357/aae373
 Grevesse, N., Asplund, M., Sauval, A. J., Scott P. 2010, *Ap&SS*, 328, 179
 Groenewegen, M. A. T. 2018, *A&A*, 619, A8
 Groenewegen, M. A. T. 2020, *A&A*, 635, A33
 Huang, C. X., Vanderburg, A., Pál, A., et al., 2020, *RNAAS*, 4, 204
 Iben, I. 1967, *ARA&A*, 5, 571
 Jurcsik, J., Hajdu, G., Catelan, M., 2018, *Acta Astr.*, 68, 341
 Kurucz R.L., 1993, A new opacity-sampling model atmosphere program for arbitrary abundances. In: Peculiar versus normal phenomena in A-type and related stars, IAU Colloquium 138, M.M. Dworetsky, F. Castelli, R. Faraggiana (eds.), A.S.P. Conferences Series Vol. 44, p.87
 Kervella, P., Arenou, F., Mignard, F., Thévenin, F., 2019, *A&A*, 623, 72
 Kovtyukh, V. V., Gorlova, N. I. 2000, *A&A*, 358, 587
 Kovtyukh, V., Lemasle, B., Chekhonadskikh, F., et al. 2016, *MNRAS*, 460, 2077
 Kovtyukh, V., Lemasle, B., Kniazev, A., et al. 2019, *MNRAS*, 488, 3211
 Kurucz R.L., 1993, Kurucz CD-ROM 13: ATLAS9, SAO, Cambridge, USA
 Kurucz R.L., Avrett E.H., 1981, *SAO Special Rep.*, 391
 Lenz, P. & Breger, M. 2005, *Communications in Asteroseismology*, 146, 53
 Luck, R. E., Kovtyukh, V. V., & Andrievsky, S. M. 2001, *A&A*, 373, 589
 Luck, R. E., Lambert, D. L., 2011, *AJ*, 142, 136
 Marconi, M., De Somma, G., Ripepi, V., et al. 2020, *ApJ*, 898, L7.
 Merc, J., Kalup, Cs., Rathour, R. S., Sánchez Arias, J. P., Beck, P. G., 2020, CoSKA, in press, arXiv:2011.08685
 Szabados, L. 1983, *Ap&SS*, 96, 185. doi:10.1007/BF00661952
 Ricker, G. R., Winn, J. N., Vanderspek, R., et al. 2015, *Journal of Astronomical Telescopes, Instruments, and Systems*, 1, 014003
 Romaniello, M., Primas, F., Mottini, M., et al. 2008, *A&A*, 488, 731
 Szegedi-Elek, E., Ábrahám, P., Wyrzykowski, Ł., et al., 2020, *ApJ*, 899, 130
 Soszyński, I., Udalski, A., Szymański, M. K., et al., 2025, *Acta Astr.*, 65, 297
 Turner, D. G., Savoy, J., Derrah, J., et al. 2005, *PASP*, 117, 207
 Turner, D. G., Abdel-Sabour Abdel-Latif, M., & Berdnikov, L. N. 2006, *PASP*, 118, 410. doi:10.1086/499501
 Turner, D. G. 2009, *Stellar Pulsation: Challenges for Theory and Observation*, 1170, 59
 Turner, D. G., Majaess, D. J., Lane, D. J., et al. 2010, *Odessa Astronomical Publications*, 23, 125
 Turner, D. G., Kovtyukh, V. V., Usenko, I. A., et al. 2013, *ApJ*, 762, L8
 Udalski, A., Soszyński, I., Pietrukowicz, P., et al. 2018, *Acta Astron.*, 68, 315. doi:10.32023/0001-5237/68.4.1
 Usenko, I. A., Miroshnichenko, A. S., Klochkova, V. G., Yushkin, M. V. 2005, *MNRAS*, 362, 1219
 Usenko, I. A. & Klochkova, V. G. 2015, *Astronomy Letters*, 41, 351
 Usenko, I. A., Kovtyukh, V. V., Miroshnichenko, A. S., Danford, S., Prendergast, P., 2018, *MNRAS*, 481, L115
 van Leeuwen, F. 2007, *Hipparcos, the New Reduction of the Raw Data: Astrophysics and Space Science Library*, Volume 350. ISBN 978-1-4020-6341-1. Springer Science+Business Media B.V., 2007

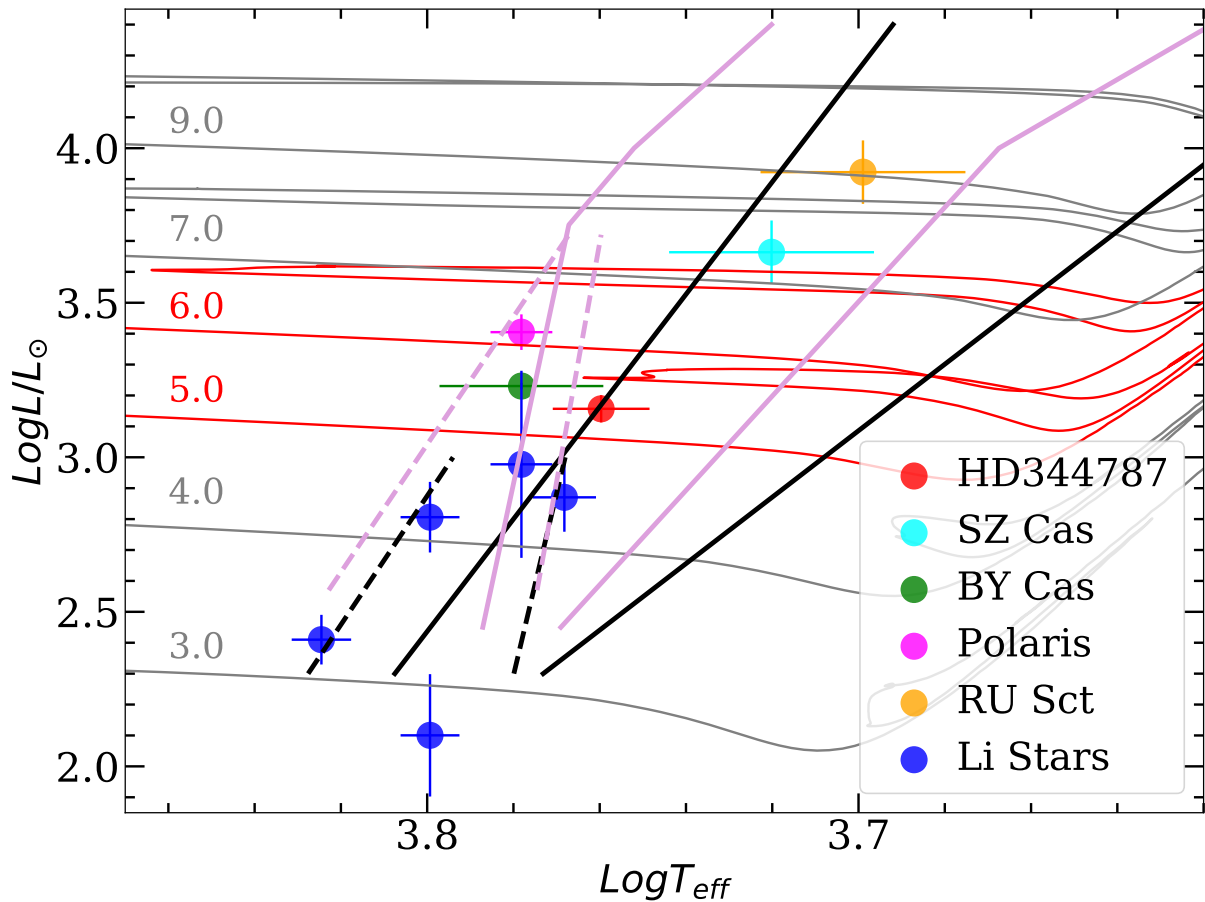


Fig. 6. HR diagram of HD 344787 and Polaris together with the other candidate first crossing DCEPs (see labels). The figure also reports MW Li-rich DCEPs from Catanzaro et al. (2020). The ISs for F (solid lines) and FO (dashed lines) DCEPs are over-plotted in black for $Z=0.02$ (De Somma et al. 2020) and in light violet for $Z=0.008$ (Bono et al. 2001). The evolutionary tracks by Bressan et al. (2012) with $Z=0.014$, $Y=0.273$ for 5 and $6 M_{\odot}$, encompassing the location of Polaris and HD 344787 in the HRD are displayed in red. Additional tracks for $3, 4, 7, 9 M_{\odot}$, are over-plotted to the data in grey.